Macromolecules

ARTICLE

pubs.acs.org/Macromolecules

Synthesis of Shape Amphiphiles Based on Functional Polyhedral Oligomeric Silsesquioxane End-Capped Poly(L-Lactide) with Diverse Head Surface Chemistry

Wen-Bin Zhang, Yiwen Li, Xiaopeng Li, Xuehui Dong, Xinfei Yu, Chien-Lung Wang, Chrys Wesdemiotis, Roderic P. Quirk,* and Stephen Z. D. Cheng*

Maurice Morton Institute and Department of Polymer Science, Department of Chemistry, The University of Akron, Akron, Ohio 44325-3909, United States

Supporting Information

ABSTRACT: This paper reports a facile, modular, and efficient approach to the synthesis of shape amphiphiles with a hydrophobic polymer chain as the tail and a polar, compact, functional polyhedral oligomeric silsequioxane (POSS) nanoparticle as the headgroup. A poly(L-lactide) (PLLA) chain was grown from monohydroxyl-functionalized heptavinyl POSS (VPOSS–OH) with controlled molecular weight and narrow polydispersity by stannous octoate-mediated ring-opening polymerization of L-lactide. To impart tunable polarity and functionality to the headgroup, various functional groups, such as carboxylic acids, hydroxyl groups, and sugars, were attached to the POSS cage in high efficiency by thiol–ene "click" chemistry, which provides a straightforward and effective approach to synthesize shape amphiphiles with diverse head surface chemistry. The polymers have been fully characterized by ^{1}H NMR, ^{13}C NMR, FT-IR spectroscopy, MALDI-TOF mass spectrometry, and size exclusion chromatography. These functional POSS can serve as versatile nanobuilding blocks in the "bottom-up" construction of nanoscale structures and assemblies that may exhibit rich self-assembling behavior and potentially useful physical properties.

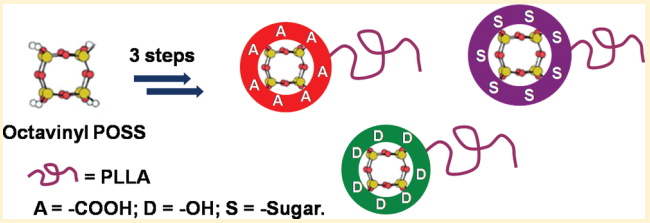

INTRODUCTION

In the "bottom up" construction of nanoscale structures and assemblies, self-assembly of nanohybrids from a library of nanobuilding blocks plays a central role.[1,2] The past 2 decades have witnessed the development of a large variety of nanobuilding blocks with different composition (organic, inorganic, biological, etc.)[3,4] and geometry/symmetry (nanospheres, cubes, discs, rods, etc).[5−7] In comparison to typical inorganic metal clusters and nanocrystals, polymers,[8] dendrimers,[9] and other molecular clusters (e.g., carborane,[10] C_{60}[11]) have also been recognized as versatile nanobuilding blocks, and they present a significant advantage as molecular nanomaterials in their well-defined molecular structures and the possibility to precisely control the molecular variables such as compositions, overall size/shape, and location of surface/interior functionalities. To date, the bottom-up approach has attracted enormous research interest both in the development of these fine-tuned nanobuilding blocks and the use of their hybrids to assemble into diverse nanostructures with desired properties.

Shape amphiphiles usually refer to molecules possessing amphiphilic features based on differences in the shape of the molecular segments.[12] Typical shape amphiphiles are composed of a functional nanobuilding block tethered with polymer chains at precise locations.[13−16] Two factors are important in the self-assembly of these shape amphiphiles: (1) shape effects of the 3D rigid and compact nanobuilding blocks that might pose different packing constraints and lead to various hierarchical structures (which can be counted as entropic contributions) and (2) important interaction effects that dominate the enthalpy contributions in the self-assembly process. Similar to small-molecule surfactants and block copolymers, they are expected to undergo microphase separation and self-assemble into a variety of nanoscale morphologies in solution.[13−15] Computer simulation has predicted asymmetric phase behaviors with far richer, interesting, hierarchical phase structures in these nanoparticle-tethered shape amphiphiles.[7,17,18] Experimentally, there are already a few reported examples, including polymers tethered with C_{60},[19] quantum dots,[20] and gold nanoparticles.[21] But there are relatively few reports on their ordered assembly in bulk or in solution, probably due to the unbalanced interactions and incommensurate shapes between the tethered head and the polymer tail that result in random aggregation. We recently reported the synthesis and self-assembly of carboxylic acid-functionalized polyhedral oligomeric silsesquioxane end-capped polystyrenes as a typical "shape amphiphile" and called it a "giant surfactant" with emphasis on its similarity to small-molecule surfactants.[14] They were found to self-assemble into various well-defined morphologies, such as spheres, cylinders, and vesicles, in selective solvents with surprisingly

Received: February 6, 2011
Revised: March 5, 2011
Published: March 25, 2011

Scheme 1. Synthesis of XPOSS−PLLA via Ring-Opening Polymerization and Thiol−Ene Click Chemistry[a]

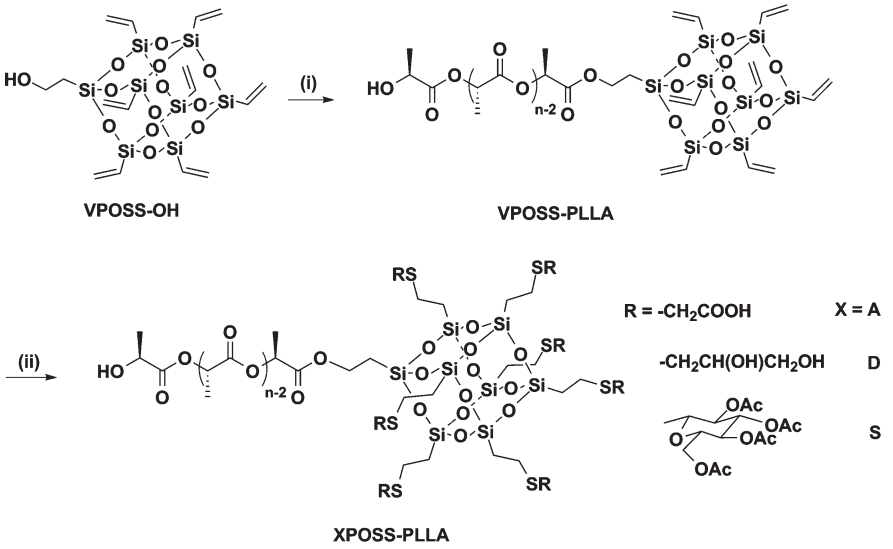

[a] (i) L-lactide, $Sn(Oct)_2$, toluene, 65 °C, conversion ~54%; (ii) RSH, DMPA, THF (or $CHCl_3$), room temperature, 15 min, 71%−89%.

highly stretched polymer chains in these assemblies, a behavior similar to small-molecule surfactants but unlike amphiphilic block copolymers. It is thus important to control the surface chemistry of the polar head of shape amphiphiles to tune these multivalent interactions between the head and the tail and the resulting self-assembly behavior. Polyvalent interactions have been recognized as a ubiquitous strategy used by Nature for the creation of a wide variety of functions not achievable with monovalent interactions.[22] Therefore, if the head of a shape amphiphile could be readily modified with multiple functional groups, it could lead to simultaneous, collective, and cooperative polyvalent interactions in a well-defined configuration. Moreover, it is also possible to impart functions to the assemblies by modifying the polar head with, for example, signal molecules for sensory or target application.[23] Therefore, a facile and efficient method for the synthesis of these shape amphiphiles with readily tunable head surface chemistry is highly desired.

POSS (polyhedral oligomeric silsequioxane), arguably the smallest silica nanoparticle with diameter around 1.0 nm, is the subject of intense research, from the synthesis and modification to conjugation with other functional materials.[24−28] Owing to the ease in its modification both on the cage structures (e.g., T_8, T_{12}) and the periphery functionality (mono-, multi-, homo- or heterofunctionalized), POSS is very promising as a versatile nanobuilding block that can act as a conformationally rigid structural scaffold to carry diverse functionalities.[29−33] This is facilitated by the use of "click" chemistry and other efficient chemical transformations,[34,35] including Cu(0)-catalyzed [3 + 2] cycloaddition between azide and alkyne,[36,37] thiol−ene reaction,[38−40] metal-catalyzed cross-coupling reactions,[32] and olefin metathesis,[41] for periphery, multiple-site functionalization. In synthesizing a POSS−polymer conjugate, direct "grafting-to" coupling of a polymer chain with an octa-functionalized POSS is usually complicated by the formation of higher addition products that require cumbersome and tedious fractionation in order to get monotethered product, as we recently reported.[14] To circumvent this disadvantage, an alternative "growing from" strategy is proposed starting from a monofunctionalized POSS initiator by polymerization. The polymerization must be compatible with the reactive groups on POSS for subsequent click functionalization. A monohydroxyl-functionalized heptavinyl POSS (VPOSS−OH, Scheme 1), developed by Feher et al.,[42] is a useful and readily available intermediate. The rich chemistry of the hydroxyl group and vinylsilsesquioxanes allows efficient and perhaps orthogonal functionalization to give various useful monofunctionalized POSS derivatives.

In this paper, we report the model synthesis of shape amphiphiles based on functional POSS-end-capped poly(L-lactide) (XPOSS−PLLA) using the sequential chain-growth and head modification strategy (Scheme 1). PLLA was grown from VPOSS−OH via tin(II) 2-ethylhexanoate-mediated ring-opening polymerization with controlled molecular weight and narrow polydispersity.[43] Diverse functionalities, such as carboxylic acids, hydroxyl groups, and glucose, were then attached to the POSS cage by thiol−ene click chemistry in high efficiency to impart tunable polarity and functionality to the headgroup. These model shape amphiphiles were synthesized to demonstrate the versatility of this method, which should be readily modified to other ring-opening monomers and periphery functionalities. In addition, facilitated by thiol−ene click chemistry, these POSS moieties may serve as versatile nanobuilding blocks for the construction of various nanohybrids that exhibit novel self-assembled structures and physical properties.

EXPERIMENTAL SECTION

Chemicals and Solvents. Trifluoromethanesulfonic acid (Aldrich, ReagentPlus, >99%), octavinyl POSS (OVPOSS, Hybrid Plastics, >97%), 2,2-dimethoxy-2-phenylacetophenone (DMPA, Acros Organics, 99%,), mercaptoacetic acid (Acros Organics, 97%,), 1-thioglycerol (Fluka, >98.0%,), and 1-thio-β-D-glucose tetraacetate (sugar−SH, Alfa Aesar, 99%) were used as received. VPOSS−OH was prepared from OVPOSS according to the literature procedure.[42] Tin(II) 2-ethylhexanoate [$Sn(Oct)_2$, Aldrich, ~95%] was fractionally distilled and diluted with anhydrous degassed toluene to make a 1 M solution before use. L-Lactide (Purac Biomaterials, >99.5%) was used after recrystallization from anhydrous toluene twice. Silica gel (VWR, 230−400 mesh) was activated by heating to 140 °C for 12 h. Dichloromethane (CH_2Cl_2, EMD, ACS grade) was purified by distillation from CaH_2. Toluene

(EMD, ACS grade) was purified by distillation from CaH_2 and then sodium, before it was stored over poly(styryl)lithium. Chloroform (EMD, ACS grade), tetrahydrofuran (THF, EMD, ACS grade), methanol (Fisher Scientific, reagent grade), and hexane (EMD, ACS grade) were used as received.

Characterizations. Size exclusion chromatographic analyses (SEC) for the synthesized polymers were performed using a Waters Breeze system with three Styragel columns at 35 °C and a refractive index detector. Samples were run at a flow rate of 0.5 mL/min with THF as the mobile phase. The molecular weight vs elution time was calibrated using narrow polydispersed polystyrene standards.

All ^{1}H and ^{13}C nuclear magnetic resonance (NMR) spectra were acquired in $CDCl_3$ (Aldrich, 99.8% D) as solvent using a Varian Mercury 300 NMR spectrometer. The ^{1}H NMR spectra were referenced to the residual proton impurities in the $CDCl_3$ at δ 7.27 ppm. ^{13}C NMR spectra were referenced to $^{13}CDCl_3$ at δ 77.00 ppm.

Infrared spectra were recorded on an Excalibur Series FT-IR spectrometer (DIGILAB, Randolph, MA) by casting polymer films on KBr plates from polymer solutions with subsequent drying. The data were processed using Win-IR software.

Matrix-assisted laser desorption/ionization time-of-flight (MALDI-TOF) mass spectra were recorded on a Bruker Ultraflex III TOF/TOF mass spectrometer (Bruker Daltonics, Billerica, MA), equipped with a Nd:YAG laser emitting at a wavelength of 355 nm. *trans*-2-[3-(4-*tert*-Butylphenyl)-2-methyl-2-propenylidene]malononitrile (DCTB, Aldrich, >99%) served as matrix and was prepared in $CHCl_3$ at a concentration of 20 mg/mL. Sodium trifluoroacetate served as cationizing agent and was prepared in MeOH/$CHCl_3$ (1/3, v/v) at a concentrations of 10 mg/mL. The matrix and NaTFA were mixed in the ratio of 10/1 (v/v). The sample preparation involved depositing 0.5 μL of matrix and salt mixture on the wells of a 384-well ground-steel plate, allowing the spots to dry, depositing 0.5 μL of each sample on a spot of dry matrix, and adding another 0.5 μL of matrix and salt mixture on top of the dry sample (sandwich method).[44] Mass spectra were measured in the reflection mode, and the mass scale was calibrated externally using the peaks of a polystyrene or PMMA standard at the molecular weight under consideration. Data analyses were conducted with Bruker's flexAnalysis software.

Molecular weight calculation was based on the integration ratio (S_1/S_2) in ^{1}H NMR spectra between the peaks at δ ~5.2 ppm (−C*H*(CH$_3$)O−) and the characteristic peaks of the POSS cage (21H at δ 6.15−5.88 ppm for VPOSS−PLLA; 14H at δ 2.70 ppm for APOSS−PLLA; 28H at δ 2.68 ppm for DPOSS−PLLA; and 84H at δ 2.02 ppm for SPOSS−PLLA), which gives the number average degree of polymerization, *n*. The molecular weight can be obtained by the summation of $M_{n,PLLA}$ ($n \times 72.04$) and M_{XPOSS} (650.0 for VPOSS, 1293.9 for APOSS, 1406.1 for DPOSS, 3198.5 for SPOSS).

General Procedure for the Polymerization. In a drybox, VPOSS−OH (0.15 g, 0.23 mmol), L-lactide (1.25 g), and 25 mL of toluene were added into a flame-dried Schlenk flask followed by the addition of Sn(Oct)$_2$ (1 M in toluene, 0.23 mL, 0.23 mmol). The mixture was taken out of the drybox, degassed twice on the high vacuum line, refilled with argon, and placed in an oil bath of 70 °C. After 16 h, the flask was cooled and the mixture was precipitated into cold methanol twice. The white solid was collected after filtration and dried at 25 °C under vacuum overnight to give VPOSS−PLLA (0.83 g, conversion: 54%). ^{1}H NMR ($CDCl_3$, 500 Hz, ppm, δ): 6.15−5.88 (m, 21H, −C*H*=C*H*$_2$), 5.18 (q, 38H, −C*H*(CH$_3$)O−), 4.36 (q, 1H, −C*H*(CH$_3$)OH), 4.28 (t, 2H, −SiCH$_2$C*H*$_2$O−), 1.59 (d, 104H, −CH(C*H*$_3$)O−), 1.22 (t, 2H, −SiC*H*$_2$CH$_2$O−). ^{13}C NMR ($CDCl_3$, 125 Hz, ppm, δ): 169.58 (−C=O), 137.10 (−CH=*C*H$_2$), 128.47 (−*C*H=CH$_2$), 69.00 (−CH(CH$_3$)O−), 16.64 (−CH(*C*H$_3$)O−). FT-IR (KBr) ν (cm^{-1}): 2996.9, 2947.2, 1759.8 (C=O), 1454.3, 1360.1, 1211.3, 1185.8, 1130.3, 1095.8 (Si−O), 1045.6, 869.9, 755.9, 690.5, 585.1. MS (MALDI-TOF): calcd monoisotopic mass for 38-mer, $C_{130}H_{178}NaO_{88}Si_8$ = 3409.8 Da, found *m*/*z* 3409.5 (100) (M·Na$^+$). $M_{n,NMR}$ = 3400 g/mol. SEC: M_w/M_n =1.13.

General Procedure for the Thiol−Ene Click Functionalization. In an open vial, VPOSS−PLLA (100 mg, 29 μmol, 1 equiv), DMPA (1 mg, 3.9 μmol, 13 mol % per polymer or 2 mol % per vinyl), and functional thiol were mixed and dissolved in solvent. After irradiation with UV 365 nm for 15 min, the mixture was purified by repeated precipitation. The collected white solid was dried under high vacuum overnight.

APOSS−PLLA. Mercaptoacetic acid (27 mg, 0.29 mmol, 10 equiv per polymer or 1.4 equiv per vinyl) and THF (2 mL) were used. After reaction, the mixture was precipitated in deionized water, cold deionized water/CH$_3$OH (v:v = 1:1), and then into cold hexane, to give a white solid (83 mg). Yield: 71%. ^{1}H NMR ($CDCl_3$, 500 Hz, ppm, δ): 5.18 (q, 52H, −C*H*(CH$_3$)O−), 4.37 (q, 1H, −C*H*(CH$_3$)OH), 4.27 (m, 2H, −SiCH$_2$C*H*$_2$O−), 3.31 (m, 14H, −SC*H*$_2$CO$_2$−), 2.70 (m, 14H, −C*H*$_2$S−), 1.59 (d, 187H, −CH(C*H*$_3$)O−), 1.21 (m, 2H, −SiC*H*$_2$CH$_2$O−), 1.06 (m, 14H, −SiC*H*$_2$−). ^{13}C NMR ($CDCl_3$, 125 Hz, ppm, δ): 175.07 (−CH$_2$*C*O$_2$H), 169.53 (−*C*=O), 69.16, 68.71 (−*C*H(CH$_3$)O−), 33.16 (−S*C*H$_2$−), 26.35 (−*C*H$_2$S−), 16.72, 16.43, 16.14 (−CH(*C*H$_3$)O−), 11.90 (−SiCH$_2$−). FT-IR (KBr) ν (cm^{-1}): 3504.7 (br, O−H), 2995.4, 2947.1, 2650.1, 1759.1 (C=O), 1454.3, 1360.4, 1288.4, 1211.3, 1185.5, 1132.3, 1095.7 (Si−O), 1045.8, 872.3, 754.2, 696.3, 553.6. MS (MALDI-TOF): calcd monoisotopic mass for 38-mer, $C_{144}H_{206}NaO_{103}S_7Si_8$ = 4053.7 Da, found *m*/*z* 4053.9 (100) (M·Na$^+$). $M_{n,NMR}$ = 5000 g/mol. SEC: M_w/M_n = 1.12.

DPOSS−PLLA. 1-Thioglycerol (27 mg, 0.29 mmol, 10 equiv per polymer or 1.4 equiv per vinyl) and THF (2 mL) were used. After reaction, the mixture was precipitated into deionized water twice and then into cold hexane, to give a white solid (100 mg). Yield: 82%. ^{1}H NMR ($CDCl_3$, 500 Hz, ppm, δ): 5.18 (q, 49H, −C*H*(CH$_3$)O−), 4.39−4.17 (m, 3H), 3.87−3.47 (m, 21H, −C*H*OHC*H*$_2$OH), 2.68 (m, 28H, −C*H*$_2$S−), 1.59 (d, 176H, −CH(C*H*$_3$)O−), 1.06 (m, br, 14H, −SiC*H*$_2$−). ^{13}C NMR ($CDCl_3$, 125 Hz, ppm, δ): 169.59 (−*C*=O), 69.20, 68.76 (−*C*H(CH$_3$)O−), 16.78, 16.49 (−CH(*C*H$_3$)O−). FT-IR (KBr) ν (cm^{-1}): 3383.8 (br, O−H), 2995.7, 2945.8, 2878.6, 1758.8 (C=O), 1454.3, 1384.6, 1360.1, 1271.1, 1211.3, 1184.7, 1130.3, 1093.2 (Si−O), 1045.8, 917.7, 871.7, 756.1, 692.4, 545.9. MS (MALDI-TOF): calcd monoisotopic mass for 38-mer, $C_{151}H_{234}NaO_{103}S_7Si_8$ = 4165.9 Da, found *m*/*z* 4166.0 (100) (M·Na$^+$). $M_{n,NMR}$ = 4900 g/mol. SEC: M_w/M_n = 1.15.

SPOSS−PLLA . 1-Thio-β-D-glucose tetraacetate (sugar−SH, 222 mg, 0.61 mmol, 21 equiv per polymer or 3 equiv per vinyl) and $CHCl_3$ (1 mL) were used. After reaction, the mixture was diluted with 10 mL of methanol and put in a refrigerator at −35 °C. The polymer precipitated out of solution in 6 h. It was collected by filtration, redissolved in minimum THF, and precipitated again into cold methanol. The final product weighed 155 mg. Yield: 89%. ^{1}H NMR ($CDCl_3$, 500 Hz, ppm, δ): 5.25−4.97 (m, 66H), 4.56 (m, 7H), 4.25 (m, 7H), 4.13 (m, 7H), 3.76 (m, 7H), 2.76 (d, 14H), 2.02 (m, 84H), 1.59 (d, 153H), 1.05 (m, 14H). ^{13}C NMR ($CDCl_3$, 125 Hz, ppm, δ): 170.44, 170.04, 169.53, 169.37, 169.24, 83.53, 73.60, 70.02, 69.16, 68.70, 67.89, 61.97, 24.02, 21.34, 20.75, 20.51, 16.72, 16.43, 16.15, 12.80. FT-IR (KBr) ν (cm^{-1}): 2995.8, 2945.6, 2258.6, 2099.3, 1755.2 (C=O), 1454.2, 1368.9, 1223.1, 1186.5, 1130.7, 1094.3 (Si−O), 1037.6, 915.0, 868.0, 734.0, 648.7. MS (MALDI-TOF): calcd monoisotopic mass for 38-mer, $C_{228}H_{318}NaO_{152}S_7Si_8$ = 5958.3 Da, found *m*/*z* 5958.0 (100) (M·Na$^+$). $M_{n,NMR}$ = 6300 g/mol. SEC: M_w/M_n = 1.16.

RESULTS AND DISCUSSIONS

Synthesis of VPOSS-PLLA. The synthetic approach outlined in Scheme 1 is very straightforward. The synthetic route was designed in an effort to fulfill the click philosophy: to construct

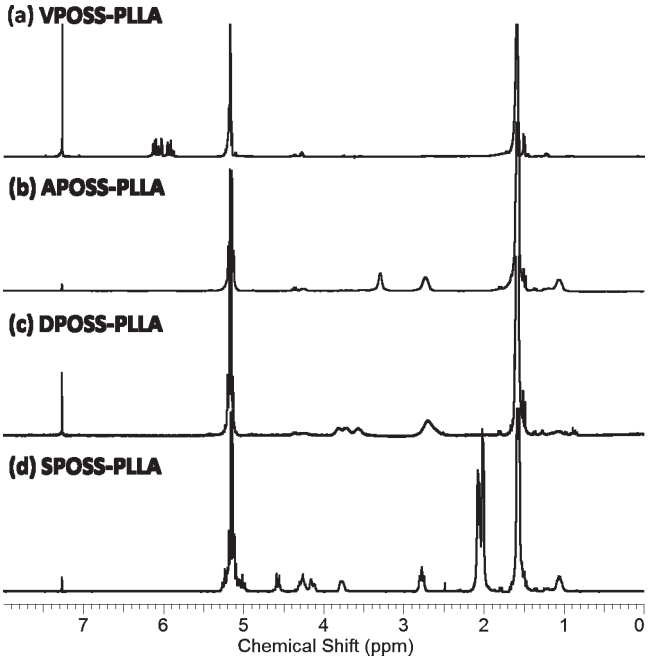

Figure 1. ^{1}H NMR spectra of (a) VPOSS−PLLA, (b) APOSS−PLLA, (c) DPOSS−PLLA, and (d) SPOSS−PLLA. The complete disappearance of the vinyl protons at 5.88−6.15 ppm and the emergence of new characteristic resonances indicate complete functionalization.

materials with complex structure and diverse function from a set of simple reactions and readily available building blocks. From the commercially available octavinyl-POSS, the monofunctionalized VPOSS−OH was readily prepared in gram quantities with all of the characterizations consistent with the literature.[42] The hydroxyl group is capable of initiating ring-opening polymerization of various monomers under different conditions. It can also be further converted to other functional initiators, such as tosylate for cationic polymerization and halide for atom transfer radical polymerization, or chain transfer agents for controlled radical polymerization. Considering the compatibility of the vinylsilsesquioxanes with different polymerization mechanisms, ring-opening polymerization of L-lactide was first chosen as the model system.[45] The method should be equally applicable to other functional lactone monomers, such as ε-caprolactone and modified lactides.[46]

The ring-opening polymerization of L-lactide under the catalysis of $Sn(Oct)_2$ has been known to proceed in a controlled fashion, giving PLLA with narrow polydispersity and controlled molecular weight.[43,47−49] The polymerization was carried at 70 °C in toluene with 1 equiv of $Sn(Oct)_2$ to VPOSS−OH. After 16 h, the polymerization was quenched and the polymer purification was achieved by repeated precipitation to remove excess monomer. The conversion of the lactide was determined to be ~54% with the target molecular weight being 3.6 kg/mol. VPOSS−PLLA is a white solid, readily soluble in common organic solvents. It was fully characterized by various techniques to confirm the structure and purity. In the ^{1}H NMR spectrum (Figure 1a), the quartet at δ 5.18 ppm and the doublet at δ 1.59 ppm are characteristic of the protons at the methine and methyl groups on the backbone, respectively.[50] The signal of vinyl protons could be clearly seen at δ 5.88−6.15 ppm, which is also affirmed by the observation of sp^2 carbons of these vinyl groups at δ 137.10 and 128.47 ppm in ^{13}C NMR spectrum (Supporting Information, Figure S1a).[50] The zoom-in view of ^{13}C NMR spectrum at the methine region (Supporting Information, Figure S2) shows a high isotacticity, indicating that little or no racemization had occurred during the polymerization process. Moreover, the protons on the two methylene groups between POSS and PLLA can be observed at δ 4.28 and 1.22 ppm, respectively, with integration ratio of 1.85:2.0, close to what is expected. The well-defined structure was confirmed by the MALDI-TOF mass spectrum (Figure 2a,b), which shows two apparent distributions. In ring-opening polymerization of L-lactide, two repeat units are generated simultaneously, leading to the formation of the major distribution. The ester-exchange reactions subsequently equilibrate the chain length, leading to both even-numbered and odd-numbered distributions.[43] Similar results have been observed both in PLLA synthesized with $Sn(Oct)_2$ or other catalyst systems.[48,51] Nevertheless, both of them actually belong to the same molecular structure. A zoom-in view is shown in Figure 2b. It is clear from the spectrum that the mass difference between all adjacent two peaks is m/z 72.0, exactly that of the lactide repeating unit. A representative peak also corresponds well with that of the calculated monoisotopic mass (Table 1). The SEC chromatogram (Figure 3) shows a symmetric, monomodal peak with narrow polydispersity (PDI = 1.13). The molecular weight observed from MALDI-TOF mass spectrum (centered at 3.5 kg/mol) is lower than that from SEC (5.9 kg/mol) but agrees well with that calculated from ^{1}H NMR (3.4 kg/mol). This is probably due to the systematic deviation of the overall elution volume of the POSS−PLLA hybrids from that of the standard polystyrenes, which can be seen in other samples as well (Table 1). The chemical structure and quantitative functionality of VPOSS−PLLA were thus unambiguously established and the sample was ready for further functionalization. Notably, no fractionation was required in the process, facilitating facile preparation of gram quantities of samples.

Model Functionalization using Thiol−Ene Click Chemistry. Thiol−ene ligation is now a well-established click process for various functionalizations.[38,39] It is particularly powerful for situations when multiple functionalization or sites of poor reactivity are involved, such as in polymers and dendrimers. Combined with unique and complex molecular scaffolds (such as POSS, fullerene, and dendrimers), it allows rapid and effective construction of functional materials of diverse molecular architectures in just a few steps.[34] In our case, in order to tune the nature of the POSS head groups and their interaction parameter with the PLLA backbone, a variety of functional groups has been successfully introduced to the POSS head. The model functionalizations were performed to introduce carboxylic acid and hydroxyl groups. The syntheses were rapid and straightforward from commercially available starting materials and the functional polymers were fully characterized by various techniques.

Hawker and co-workers[52,53] have demonstrated that the reaction between periphery vinyl groups and mercaptoacetic acid is a convenient way to modify dendrimer surfaces with carboxylic acids. Our previous work has also proved the high efficiency of radical addition of mercaptoacetic acid to vinylsilsesquioxanes in the synthesis of the polystyrene analogue, APOSS−PS.[14] The first trial in POSS−PLLA was also based on this reaction. The successful ligation was proven by the complete disappearance of POSS vinyl proton resonances at δ 5.88−6.15 ppm and the appearance of the two thio-ether methylene linkages at δ 3.31 and 2.70 ppm in the ^{1}H NMR spectrum (Figure 1b). The chemical shifts agree well with that of the reported analogue

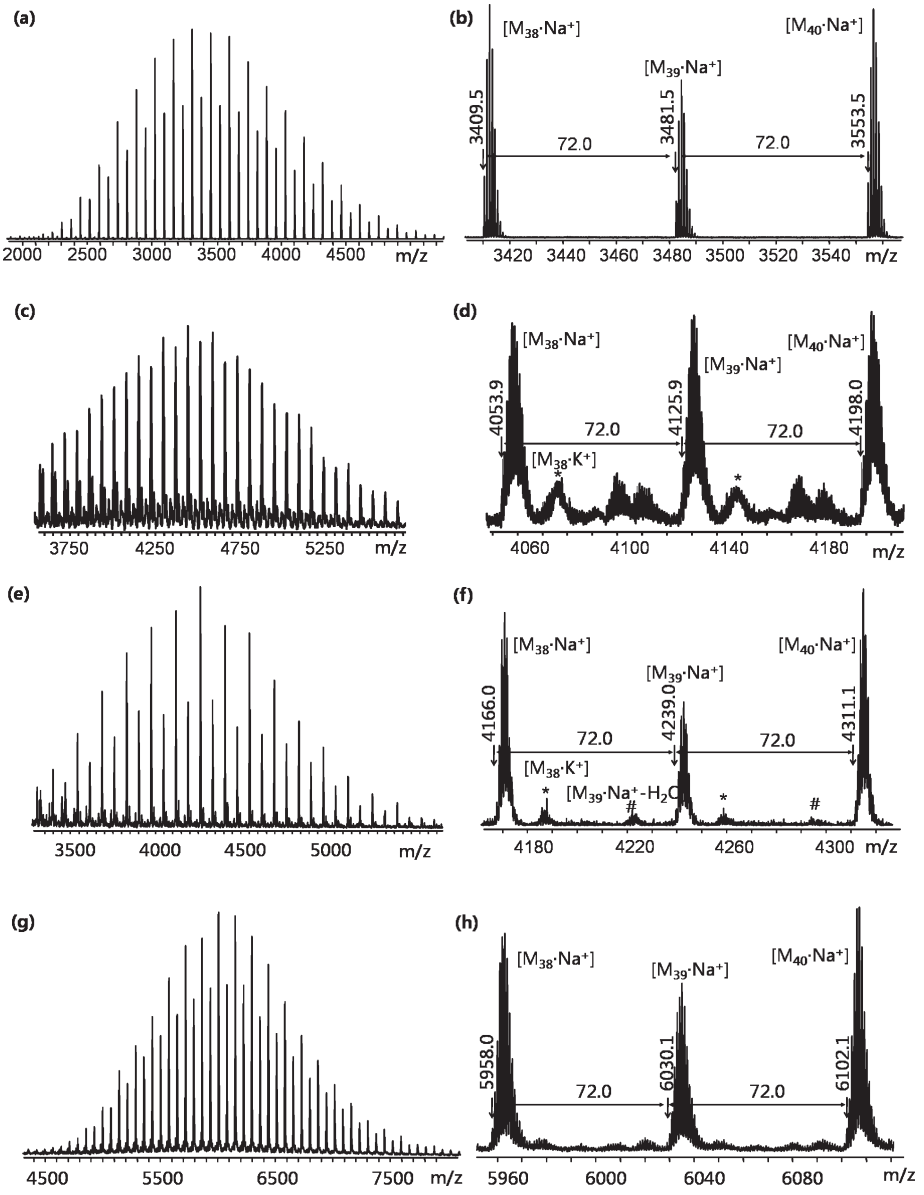

Figure 2. MALDI-TOF mass spectra of VPOSS−PLLA (a, b), APOSS−PLLA (c, d), DPOSS−PLLA (e, f), and SPOSS−PLLA (g, h), among which panels a, c, e, and g are overviews of the spectra and panels b, d, f, and h are the zoom-in view of the spectra at specific mass range to show the mass difference between two neighboring peaks and their monoisotopic pattern.

(APOSS−PS).[14] Similarly, in the ^{13}C NMR spectrum (Supporting Information, Figure S1b), no vinyl sp^2 carbons could be observed while four new peaks appeared at δ 11.90, 26.35, 33.16, and 175.07 ppm, consistent with the formation of $-SiCH_2CH_2SCH_2CO_2H$ on POSS. Due to the small size of the functional group, the SEC trace of APOSS−PLLA (Figure 3) only shows a slight shift to lower retention volume; however, the peak remains narrow and symmetric, basically the same as the starting material VPOSS−PLLA. The corresponding mass spectrum (Figure 2c,d) shows a APOSS−PLLA distribution centered at ~4500 Da, which confirms the formation of this product by the matching of the observed monoisotopic mass to the calculated ones (e.g., m/z 4053.9 observed vs 4053.7 Da calculated for 38-mer; see also Table 1). Meanwhile, several minor distributions of low intensity (Figure 2d) and a low-mass distribution of PLLA, $HO-(CH(CH_3)COO)_n-H$ (Na^+ adducts, data not shown) were observed, which could probably be due to the fragmentation upon MALDI.

Hydroxyl groups are basically neutral and hydrophilic. Molecules possessing multiple hydroxyl groups usually play interesting roles in biological systems, and prime examples are the carbohydrates. Further transformation of hydroxyl groups also allows construction of more complex structures, such as dendrimers.[52] In self-assembly, the strong hydrogen-bond-forming ability of hydroxyls leads to intriguing and stable morphologies that, unlike carboxylic acids, are not easily influenced by the pH of the solution. Reacting VPOSS−PLLA with 1-thioglycerol should install 14 hydroxyl groups into the POSS head at one time. Following an identical procedure as for APOSS−PLLA, the DPOSS−PLLA was prepared by the thiol−ene reaction with 10 equiv of 1-thioglycerol. In the ^1H NMR spectrum, the new resonance at δ 2.68 ppm is characteristic of the protons on the two

Table 1. Summary of Characterizations for POSS−PLLA

sample	molecular formula[a]	M (calc)[a] (Da)	m/z (obs)	$M_{n,NMR}$ (g/mol)	$M_{n,SEC}$ (g/mol)	PDI
VPOSS−PLLA	$C_{130}H_{178}NaO_{88}Si_8$	3409.8	3409.5	3.4K	5.9K	1.13
APOSS−PLLA	$C_{144}H_{206}NaO_{103}S_7Si_8$	4053.7	4053.9	5.0K	6.3K	1.12
DPOSS−PLLA	$C_{151}H_{234}NaO_{103}S_7Si_8$	4165.9	4166.0	4.9K	6.0K	1.15
SPOSS−PLLA	$C_{228}H_{318}NaO_{152}S_7Si_8$	5958.3	5958.0	6.3K	8.0K	1.16

[a] The molecular formula and molecular monoisotopic mass are based on 38-mer with a sodium ion ($M\cdot Na^+$).

methylene groups adjacent to sulfur atom, and the resonance at δ 3.47−3.87 ppm can be assigned to the protons on the carbons bonded to the oxygens [$-CH(OH)CH_2OH$]. There is no alkene proton signal in the range of δ 6.15−5.88 ppm, suggesting complete functionalization. The MALDI-TOF mass spectrum also provides evidence for complete functionalization and a well-defined structure (Figure 2e,f). Similar to that of the starting material, two apparent distributions could be seen in Figure 2c for DPOSS−PLLA as well, which are actually assignable to the same chemical structure (Table 1), since their mass difference is that of a repeating unit (Figure 2f). There are two additional minor distributions (* and #) of very small intensity. The one, denoted by * and represented by the peak with monoisotopic mass at m/z 4182.0, has a molecular weight gain of ~16 Da compared to the main distribution (m/z 4166.0 for 38-mer), while the other, denoted by # with characteristic monoisotopic mass at m/z 4220.2, has a loss of m/z ~18 compared to the main distribution (m/z 4238.1 for 38-mer). It is proposed that the former might correspond to the molecules ionized with potassium ($M\cdot K^+$) and/or from minor oxidized molecules and the latter is due to the loss of H_2O during the laser ionization process, which is common for MALDI-TOF analysis of molecules with multiple hydroxyl groups. The presence of multiple hydroxyl groups in the molecule is also evidenced by the broad absorption centered at ~3384 cm^{-1} in the FT-IR spectrum (Supporting Information, Figure S3), characteristic of hydrogen-bonded hydroxyl groups.[50] In SEC (Figure 3), the elution profile of DPOSS−PLLA is basically the same as that of VPOSS−PLLA, since the modification with these small functional groups on such a rigid POSS scaffold does not affect the overall hydrodynamic volume very much. All of the evidence supports the formation of DPOSS−PLLA as proposed. Therefore, the model functionalization with small functional groups is conveniently achieved, yielding shape amphiphiles with a polar head functionalized with seven carboxylic acids or 14 hydroxyl groups. On the basis of the convincing results, it was of interest to extend this method to other polar functionalities to test the scope of the method and explore the possibility to install additional functions.

Preparation of Shape Amphiphile with a Glycocluster Head. To further adapt the structure of shape amphiphiles to impart function, it was of interest to investigate the use of glycocluster as a polar head. It is known that carbohydrates are heavily involved in various biological processes, such as cell signaling, energy storage, and viral and bacterial infections.[54] In particular, oligosaccharides that are clustered in multiantennary configurations constitute signal transductors between cell and extracellular matrices.[55] Actually, only the simultaneous, synergestic, and cooperative interactions between multiple carbonhydrate ligands and proteins can achieve sufficient specificity and selectivity in the binding and recognition process, an effect known as the "glycocluster effect".[54] Compared to dendritic structures, the POSS cage provides a versatile and convenient platform for multifunctionlization with a predefined, rigid configuration and high symmetry.[40] Its derivatization into

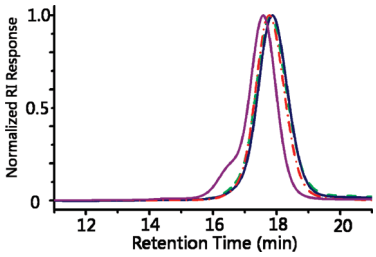

Figure 3. SEC overlay of VPOSS−PLLA (shown in blue, solid curve), APOSS−PLLA (red, dotted curve), DPOSS−PLLA (green, dotted curve), and SPOSS−PLLA (purple, solid curve).

glycoclusters has been achieved both by standard amidation[56] and thiol−ene reaction.[40] The resulting conjugate exhibited ~200 times stronger inhibition effects in lectin binding study than that from free lactose. Similar glycoclusters have also been achieved on the basis of the C_{60} structural scaffold using the Cu(0)-catalyzed Huisgen 1,3-dipolar cycloaddition of azides and alkynes.[57] It was thus of great interest to use these glycoclusters as the polar head in shape amphiphiles. It was anticipate that these sugar-ball-headed shape amphiphiles with polylactide tails would be promising candidates as potential target drug delivery vehicles in biomedical engineering.

The 1-thio-β-D-glucose tetraacetate (sugar−SH) is commercially available and was used as the model glyco-thiol to prepare SPOSS−PLLA. At first, when only 10 equiv of sugar−SH was used, a strong shoulder peak could be observed in SEC of the product (Supporting Information, Figure S4), suggesting the formation of higher molecular weight fractions that are most likely polymeric dimers from the radical coupling of the intermediates. This is common for polymers of higher molecular weight and for thiol compounds of large size.[53] In this case, the thiol in sugar−SH is linked directly to a glucose ring without a spacer and thus imposes considerable steric hindrance, both for the higher additions of sugar−SH and for the abstraction of hydrogen from −SH by a polymeric radical. The situation is worse in the absence of a large excess of sugar−SH. Indeed, when sugar−SH was used in 21 equiv at high concentration, the formation of high molecular weight fractions could be suppressed to a minimum (Supporting Information, Figure S4). In contrast, the use of 10 equiv of thiol is already sufficient for complete functionalization without formation of trace high molecular weight fractions in APOSS−PLLA and DPOSS−PLLA. Although a large excess of sugar−SH is required, it was found that most of the excess could be recovered after reaction. It is also anticipated that the situation could be alleviated with the use of less sterically hindered, primary thiols (available in one step from amino-terminated glycosides).[40]

The successful preparation of SPOSS−PLLA was proved by ^1H NMR, ^{13}C NMR, FT-IR, and MALDI-TOF mass spectrometry. The proton at −SH in sugar−SH at δ 2.32 ppm and the alkene

protons at VPOSS−PLLA at δ 5.88−6.15 ppm disappeared in the ^{1}H NMR spectrum (Figure 1d). The newly formed thiol ether bond is evidenced by its methylene proton resonance at δ 2.76 ppm. The C1 glucose proton adjacent to the thio-ether bond could not be clearly distinguished because its chemical shift (~5.25 ppm) overlaps with that of the backbone methine proton (5.18 ppm). The resonances assigned to the other protons of the glucose ring remain at the same chemical shifts but lose resolution and broaden. The carbon atoms on the glucose scaffold were also observed by ^{13}C NMR spectroscopy (Supporting Information, Figure S1d), including those around δ 170 ppm for acetyl carbonyls and δ 83 ppm for the C1 carbon bonded to sulfur. In the corresponding SEC chromatogram (Figure 3), the peak completely shifts to a lower elution volume due to the large increase in molecular weight. A small shoulder peak is present, as discussed previously. As a result, the polydispersity index slightly increased to 1.16. Despite the existence of trace amounts of higher molecular weight fractions, the MALDI-TOF mass spectrum shows unequivocally the distribution of molecular weights in accordance to the proposed structure (Figure 2g,h and Table 1). No high molecular weight product was actually observed, because they are usually more difficult to ionize than low molecular weight fractions. Owing to the large differences in molecular weight (~12 vs ~6 kDa) and relative contents (high molecular weight fraction ~10% from SEC by peak deconvolution), the laser might selectively ionize the low molecular weight fractions. Nevertheless, the spectrum clearly shows the homogeneity and well-defined structure of SPOSS−PLLA at that molecular weight range.

CONCLUSIONS

In summary, we have demonstrated a facile approach to prepare shape amphiphiles (XPOSS−PLLA) with diverse head surface chemistry via the combination of ring-opening polymerization and thiol−ene click chemistry. The polymers comprise a poly(L-lactide) chain tethered with a carboxylic-acid-functionalized POSS head (APOSS−PLLA), with a 14-hydroxyl-functionalized POSS head (DPOSS−PLLA), or with a glycocluster head (SPOSS−PLLA). The synthesis fulfills a click philosophy in material construction, namely, to build diverse and complex structures/functions from a simple set of highly efficient chemical transformations. The method should be easily extended to other polymers (e.g., PCL) and other functional groups (e.g., charged, or fluorous functional groups) for fine-tuning of the interaction parameters in shape amphiphiles. The shape amphiphiles reported in this study serve as model compounds to demonstrate the versatility of the method and to explore their self-assembly behaviors. Notably, these functional POSS heads can be used as versatile nanobuilding blocks to be incorporated into other molecular structures for bottom-up construction of mesoscopic nanomaterials via self-assembly. The relevant work on the synthesis, self-assembly, and application of various shape amphiphiles based on POSS is currently under intense investigation in our laboratory.

ASSOCIATED CONTENT

Supporting Information. Detailed characterization data, including ^{13}C NMR spectra, FT-IR spectra, and SEC traces. This material is available free of charge via the Internet at http://pubs.acs.org.

AUTHOR INFORMATION

Corresponding Author

*Tel: + 1 330 972 6931. Fax: + 1 330 972 8626. E-mail: rpquirk@uakron.edu (R.P.Q.), scheng@uakron.edu (S.Z.D.C.).

ACKNOWLEDGMENT

This work was supported by NSF (DMR-0906898, DMR-0821313, CHE-1012636). The authors acknowledge Mr. Pengzhan Fei, Mr. Yuqing Liu, and Prof. Kevin A. Cavicchi for the help with size exclusion chromatography in their laboratory. W.-B.Z. acknowledges Lubrizol Corp. for a fellowship.

REFERENCES

(1) Niemeyer, C. M.; Mirkin, C. A. *Nanobiotechnology: Concepts, Applications and Perspectives*; Wiley-VCH: Weinheim, 2004.
(2) Lehn, J. M. *Supramolecular Chemistry: Concepts and Perspectives*; VCH: Weinheim; New York, 1995.
(3) Patil, A. J.; Mann, S. *J. Mater. Chem.* **2008**, *18*, 4605–4615.
(4) Steinmetz, N. F.; Bize, A.; Findlay, K. C.; Lomonossoff, G. P.; Manchester, M.; Evans, D. J.; Prangishvili, D. *Adv. Funct. Mater.* **2008**, *18*, 3478–3486.
(5) Kitaev, V. *J. Mater. Chem.* **2008**, *18*, 4745–4749.
(6) Jun, Y. W.; Seo, J. W.; Oh, S. J.; Cheon, J. *Coordin. Chem. Rev.* **2005**, *249*, 1766–1775.
(7) Glotzer, S. C.; Solomon, M. J. *Nat. Mater.* **2007**, *6*, 557–562.
(8) Kickelbick, G. *Prog. Polym. Sci.* **2003**, *28*, 83–114.
(9) Newkome, G. R. *Dendritic Macromolecules: Concepts, Syntheses, Perspectives*; Wiley-VCH, 1997.
(10) Hawthorne, M. F.; Farha, O. K.; Julius, R.; Ma, L.; Jalisatgi, S. S.; Li, T. J.; Bayer, M. J. *ACS Symp. Ser.* **2006**, *917*, 312–324.
(11) Prassides, K.; Alloul, H. *Fullerene-Based Materials: Structures and Properties*; Springer: New York, 2004.
(12) Date, R. W.; Bruce, D. W. *J. Am. Chem. Soc.* **2003**, *125*, 9012–9013.
(13) Reynhout, I. C.; Cornelissen, J. J. L. M.; Nolte, R. J. M. *Acc. Chem. Res.* **2009**, *42*, 681–692.
(14) Yu, X.; Zhong, S.; Li, X.; Tu, Y.; Yang, S.; Van Horn, R. M.; Ni, C.; Pochan, D. J.; Quirk, R. P.; Wesdemiotis, C.; Zhang, W.-B.; Cheng, S. Z. D. *J. Am. Chem. Soc.* **2010**, *132*, 16741–16744.
(15) Zhang, Z. L.; Horsch, M. A.; Lamm, M. H.; Glotzer, S. C. *Nano Lett.* **2003**, *3*, 1341–1346.
(16) Glotzer, S. C.; Horsch, M. A.; Iacovella, C. R.; Zhang, Z. L.; Chan, E. R.; Zhang, X. *Curr. Opin. Colloid Interface Sci.* **2005**, *10*, 287–295.
(17) Zhang, X.; Chan, E. R.; Glotzer, S. C. *J. Chem. Phys.* **2005**, *123*, 184718.
(18) Iacovella, C. R.; Horsch, M. A.; Zhang, Z.; Glotzer, S. C. *Langmuir* **2005**, *21*, 9488–9494.
(19) Zhang, W. B.; Tu, Y.; Ranjan, R.; Van Horn, R. M.; Leng, S.; Wang, J.; Polce, M. J.; Wesdemiotis, C.; Quirk, R. P.; Newkome, G. R.; Cheng, S. Z. D. *Macromolecules* **2008**, *41*, 515–517.
(20) Westenhoff, S.; Kotov, N. A. *J. Am. Chem. Soc.* **2002**, *124*, 2448–2449.
(21) Parak, W. J.; Pellegrino, T.; Micheel, C. M.; Gerion, D.; Williams, S. C.; Alivisatos, A. P. *Nano Lett.* **2003**, *3*, 33–36.
(22) Mammen, M.; Choi, S. K.; Whitesides, G. M. *Angew. Chem., Int. Ed.* **1998**, *37*, 2755–2794.
(23) Wobus, U.; Weber, H. *Biol. Chem.* **1999**, *380*, 937–944.
(24) Lickiss, P. D.; Rataboul, F. *Adv. Organomet. Chem.* **2008**, *57*, 1–116.
(25) Pielichowski, K.; Njuguna, J.; Janowski, B.; Pielichowski, J. *Adv. Polym. Sci.* **2006**, *201*, 225–296.
(26) Wu, J.; Mather, P. T. *Polym. Rev.* **2009**, *49*, 25–63.
(27) Haxton, K. J.; Morris, R. E. *Adv. Silicon Sci.* **2009**, *2*, 121–1391.

(28) Cordes, D. B.; Lickiss, P. D.; Rataboul, F. *Chem. Rev.* **2010**, *110*, 2081–2173.
(29) Laine, R. M.; Zhang, C. X.; Sellinger, A.; Viculis, L. *Appl. Organomet. Chem.* **1998**, *12*, 715–723.
(30) Laine, R. M. *J. Mater. Chem.* **2005**, *15*, 3725–3744.
(31) Sulaiman, S.; Bhaskar, A.; Zhang, J.; Guda, R.; Goodson, T.; Laine, R. M. *Chem. Mater.* **2008**, *20*, 5563–5573.
(32) Roll, M. F.; Asuncion, M. Z.; Kampf, J.; Laine, R. M. *ACS Nano* **2008**, *2*, 320–326.
(33) Laine, R. M.; Roll, M.; Asuncion, M.; Sulaiman, S.; Popova, V.; Bartz, D.; Krug, D. J.; Mutin, P. H. *J. Sol−Gel Sci. Technol.* **2008**, *46*, 335–347.
(34) Kolb, H. C.; Finn, M. G.; Sharpless, K. B. *Angew. Chem., Int. Ed.* **2001**, *40*, 2004–2021.
(35) Sumerlin, B. S.; Vogt, A. P. *Macromolecules* **2010**, *43*, 1–13.
(36) Meldal, M.; Tornoe, C. W. *Chem. Rev.* **2008**, *108*, 2952–3015.
(37) Zhang, W. A.; Muller, A. H. E. *Macromolecules* **2010**, *43*, 3148–3152.
(38) Kade, M. J.; Burke, D. J.; Hawker, C. J. *J. Polym. Sci., Part A: Polym. Chem.* **2010**, *48*, 743–750.
(39) Hoyle, C. E.; Bowman, C. N. *Angew. Chem., Int. Ed.* **2010**, *49*, 1540–1573.
(40) Gao, Y.; Eguchi, A.; Kakehi, K.; Lee, Y. C. *Org. Lett.* **2004**, *6*, 3457–3460.
(41) Feher, F. J.; Soulivong, D.; Eklund, A. G.; Wyndham, K. D. *Chem. Commun.* **1997**, 1185–1186.
(42) Feher, F. J.; Wyndham, K. D.; Baldwin, R. K.; Soulivong, D.; Lichtenhan, J. D.; Ziller, J. W. *Chem. Commun.* **1999**, 1289–1290.
(43) Dechy-Cabaret, O.; Martin-Vaca, B.; Bourissou, D. *Chem. Rev.* **2004**, *104*, 6147–6176.
(44) Gunes, K.; Isayev, A. I.; Li, X. P.; Wesdemiotis, C. *Polymer* **2010**, *51*, 1071–1081.
(45) Leemhuis, M.; van Nostrum, C. F.; Kruijtzer, J. A. W.; Zhong, Z. Y.; ten Breteler, M. R.; Dijkstra, P. J.; Feijen, J.; Hennink, W. E. *Macromolecules* **2006**, *39*, 3500–3508.
(46) Brunelle, D. J. *Ring-Opening Polymerization: Mechanisms, Catalysis, Structure, Utility*. Hanser Publishers: Munich, 1993.
(47) Kowalski, A.; Duda, A.; Penczek, S. *Macromolecules* **2000**, *33*, 7359–7370.
(48) Kowalski, A.; Duda, A.; Penczek, S. *Macromolecules* **2000**, *33*, 689–695.
(49) Kowalski, A.; Libiszowski, J.; Biela, T.; Cypryk, M.; Duda, A.; Penczek, S. *Macromolecules* **2005**, *38*, 8170–8176.
(50) Silverstein, R. M.; Webster, F. X.; Kiemle, D. J. *Spectrometric Identification of Organic Compounds*, 7th ed.; John Wiley & Sons: Hoboken, NJ, 2005.
(51) Zhang, L.; Nederberg, F.; Messman, J. M.; Pratt, R. C.; Hedrick, J. L.; Wade, C. G. *J. Am. Chem. Soc.* **2007**, *129*, 12610–12611.
(52) Killops, K. L.; Campos, L. M.; Hawker, C. J. *J. Am. Chem. Soc.* **2008**, *130*, 5062–5064.
(53) Antoni, P.; Robb, M. J.; Campos, L.; Montanez, M.; Hult, A.; Malmstrom, E.; Malkoch, M.; Hawker, C. J. *Macromolecules* **2010**, *43*, 6625–6631.
(54) Dwek, R. A. *Chem. Rev.* **1996**, *96*, 683–720.
(55) Chabre, Y. M.; Roy, R. *Adv. Carbohydr. Chem. Biochem.* **2010**, *63*, 165–393.
(56) Feher, F. J.; Wyndham, K. D.; Knauer, D. J. *Chem. Commun.* **1998**, 2393–2394.
(57) Nierengarten, J. F.; Iehl, J.; Oerthel, V.; Holler, M.; Illescas, B. M.; Munoz, A.; Martin, N.; Rojo, J.; Sanchez-Navarro, M.; Cecioni, S.; Vidal, S.; Buffet, K.; Durka, M.; Vincent, S. P. *Chem. Commun.* **2010**, *46*, 3860–3862.